DOI: 10.63527/1607-8829-2024-1-2-23-33

V.A. Holovatsky, *DSc. (Phys-Math)*
I.V. Holovatskyi,
N.H. Holovatska

Yuriy Fedkovych Chernivtsi National University,
2 Kotsiubynskyi str., Chernivtsi, 58012, Ukraine
e-mail: v.holovatsky@chnu.edu.ua

ELECTRIC FIELD EFFECT ON THE INTRABAND OPTICAL ABSORPTION SPECTRA IN OF THE LENS-SHAPED QUANTUM DOTS

The study investigates the influence of an electric field on the energies, oscillator strengths, and absorption coefficients of intraband quantum transitions of an electron in lens-shaped quantum dots. The problem was solved within the framework of the effective mass approximation for two models of lens-shaped quantum dots: a spherical segment and a hemiellipsoid. For both models, the research was conducted using the finite element method in the COMSOL Multiphysics system. Additionally, for the second quantum dot model, exact solutions of the Schrödinger equation were obtained, based on which the influence of the electric field was studied using the diagonalization method. It was shown that the energies and oscillator strengths of intraband quantum transitions obtained by different methods and for different models of lens-shaped quantum dots coincide with high accuracy.

Key words: lens-shaped quantum dot, ellipsoidal quantum dot, absorption coefficient.

Introduction

Molecular beam epitaxy and colloidal synthesis are currently the main methods for growing quantum dots. Each of these methods has its own advantages and disadvantages. The primary advantages of colloidal synthesis include low cost and fast growth, which make this method suitable for industrial-scale applications. Additionally, one of the advantages of colloidal synthesis is the ability to produce quantum dots with a precise spherical shape. This makes them particularly useful for applications where high uniformity and predictability of properties are required, such as in biomedical markers, LEDs, and other optoelectronic devices. The simple geometric shape of colloidal quantum dots simplifies theoretical studies of their energy spectrum, even in cases of complex internal spherically symmetric structures and the presence of external fields [1 – 4]. On the other hand, the spherical shape complicates the integration of quantum dots into nanoelectronic circuits, where precise alignment and positioning of nanostructures are often necessary. For example, in transistors and logic elements, it is important to have controlled interfaces and contacts, which are more challenging to achieve with spherical dots. Spherical quantum dots may have less contact with the substrate, which can lead to instability in electrical properties and reduced charge transfer efficiency in photovoltaic devices.

For applications in nanoelectronics and digital technologies, quantum dots of other shapes are often used. For example, cylindrical, pyramidal, or prismatic quantum dots provide reliable contact with the surface on which they are grown, which is important for the stability of the electrical properties of nanostructures. Hemispherical or lens-shaped quantum dots combine the advantages of spherical dots for

optical applications with improved properties for electronic applications due to their flat base, which ensures contact with the substrate.

Lens-shaped quantum dots of various semiconductor compositions are obtained through self-organization methods in molecular beam or droplet epitaxy [5 – 6]. Due to their unique physical properties, they find applications in photonic integrated circuits, photodetectors, biomedical applications, as well as in the creation of high-efficiency LEDs and lasers. Additionally, quantum dots hold potential for use in quantum computing, where they can serve as qubits, the fundamental elements of quantum computers. They are used as quantum light sources for generating single and entangled photons, which have important applications in secure quantum communication and optical quantum computing [7].

Control over the size, shape, and arrangement of quantum dots allows for tuning their spectral characteristics, opening up new possibilities for the development of advanced optoelectronic devices. Thus, research and improvement of quantum dot growth methods are crucial for the advancement of modern technologies. Studying the effects of various factors on their properties, particularly the electric field, not only deepens our understanding of fundamental physical processes but also enables the creation of new, more efficient devices for various fields of science and technology. In particular, the results of such studies are of great importance for thermoelectrics and thermophotoelectrics. The study of the effect of electric field on intraband absorption in lenticular quantum dots can contribute to the development of nanostructures capable of increasing the efficiency of thermal energy conversion into light or electricity. In thermoelectric devices, such quantum dots can be used to optimize the thermal conductivity of materials and improve energy efficiency [8 – 9].

Theoretical studies of the optical properties of lens-shaped quantum dots have been carried out by many authors using various methods [10 – 12]. In the specific case of hemispherical quantum dots, it is possible to obtain an exact energy spectrum and wave functions expressed through spherical Bessel functions that satisfy the boundary conditions of the problem. This set of solutions serves as an orthonormal basis for investigating the impact of various perturbations using the matrix method. For example, in [10], Shu-Dong Wu used a similar method to study the effect of an electric field (Stark effect) on the exciton spectrum in hemispherical *InAs* quantum dots. He found a highly anisotropic Stark redshift in the exciton energy. Lo´pez Gondar and colleagues investigated the linear and nonlinear effects of a magnetic field on the energy spectrum and wave functions of electrons in hemispherical quantum dots [11]. In [12], the influence of an electric field on the oscillator strengths of quantum transitions in *CdSe*/*ZnTe* type-II core-shell hemispherical quantum dots was studied. The calculations were performed using two different methods: the matrix method with an orthonormal basis of wave functions and the finite element method. The study showed that the results obtained by different methods closely agree with high accuracy across various values of electric field intensity.

For theoretical studies of the optical properties of lens-shaped quantum dots, various numerical methods for solving the Schrödinger equation are most commonly used [10 – 11]. For example, the finite element method within the integrated platform for numerical modeling, COMSOL Multiphysics, allows for the specification of various quantum dot shapes for which analytical solutions are not possible.

In this work, we calculate the impact of an electric field on the electron energy spectrum in a lens-shaped quantum dot, including energy levels, oscillator strengths, and selection rules for intersubband quantum transitions. The study is conducted using two models of a lens-shaped quantum dot: a spherical segment and a hemiellipsoid. It is worth noting that for the second model, there are exact solutions to the Schrödinger equation in the form of elliptic functions. This allows for the construction of an orthonormal basis and the investigation of the electric field's effect on the electron energies and wave functions in the nanostructure using the matrix method.

1. Theory

Let's consider two models of a lens-shaped quantum dot: a spherical segment and a hemiellipsoid, which have the same height and volume (Fig. 1).

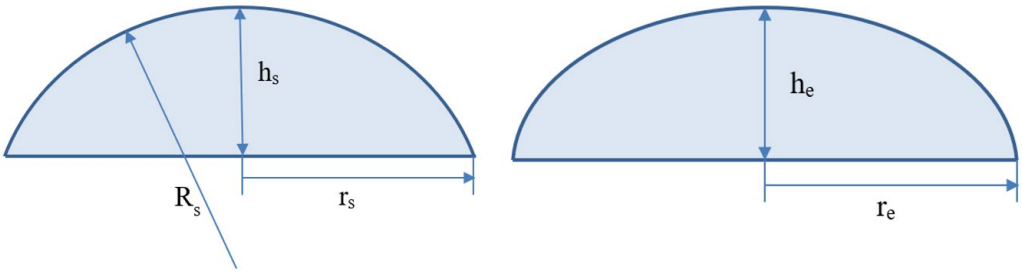

Fig. 1. Geometric diagram of the lens-shaped quantum dot: a) spherical segment; b) hemiellipsoid.

The volume of the spherical segment V_s is determined by its height h_s and the radius of its base r_s

$$V_s = \frac{\pi}{6} h(3r_s^2 + h_s^2). \tag{1}$$

The volume of half of a flattened spheroid (an ellipsoid with semi-axes $a = b = r_e$, $c = h_s$) is given by

$$V_e = \frac{2\pi}{3} r_e^2 h_e. \tag{2}$$

Given the ratio between the semi-axes of the spheroid $\chi = r_e/h_e$, and assuming $h_e = h_s$, to ensure the volumes of both quantum dot models are equal, the radius of the base of the spherical segment is determined by the expression

$$r_s = h\sqrt{(4\chi^2 - 1)/3}\ . \tag{3}$$

As seen from (3), for $\chi > 1$, we obtain $r_s > r_e$.

To find the energy spectrum and wave functions of an electron in a lens-shaped quantum dot placed in a uniform electric field directed along the Oz axis, which is perpendicular to the base of the quantum dot, it is necessary to solve the Schrödinger equation with the Hamiltonian

$$H = -\frac{\hbar^2}{2m^*}\nabla^2 + eFz + U(\vec{r}) \tag{4}$$

$$U(\vec{r}) = \begin{cases} 0, & inner\ of\ the\ QD \\ V_0, & outer\ of\ the\ QD \end{cases} \tag{5}$$

In the absence of an electric field and with $V_0 = \infty$, similar to hemispherical quantum dots [9], the model of a half-spheroid quantum dot has exact solutions to the Schrödinger equation. The electron energies in such a quantum dot can be found within the energy spectrum of an electron in an oblate spheroid [13 – 15], where the wave function satisfies the boundary conditions, meaning it is equal to zero not only on the surface of the ellipsoid but also in the XOY plane.

The set of wave functions $\Phi_{nlm}(\vec{r})$, which satisfy the specified boundary conditions, forms the basis on which the matrix method is used to obtain the solutions to equation (4)

$$\psi_{jm}(\vec{r}) = \sum_{n,l} c_{nlm}^{jm} \Phi_{nlm}(\vec{r}). \tag{7}$$

Based on the energy spectrum and the wave functions of the electron ψ_{jm}, the energies of intraband quantum transitions of the electron in a lens-shaped quantum dot in an electric field $E_{fi} = E_f - E_i$ and their oscillator strengths can be calculated.

$$F_{fi} = 2m^* E_{fi} \left|M_{fi}\right|^2 / \hbar^2 , \tag{8}$$

where $M_{fi} = \langle \psi_f | e\, z | \psi_i \rangle$ is the electric dipole moment of the quantum transition. The calculation results of the oscillator strengths for different quantum transitions will allow us to establish selection rules and their dependence on the electric field. For the oscillator strengths of quantum transitions from the ground to various excited quantum states, the following relationship must hold

$$\sum_f F_{1f} = 1, \tag{9}$$

This relationship is called the Thomas-Reich-Kuhn rule of sums. This allows you to control the accuracy of numerical calculations.

To calculate the change in the optical absorption coefficient due to intersubband transitions, we assume the interaction of a polarized monochromatic electromagnetic field with an ensemble of quantum dots. The calculation of the linear optical absorption coefficient corresponding to intersubband optical transitions is performed using the expression obtained within the framework of the compact density matrix approach.

$$\alpha^{(1)}(\omega) = \sqrt{\frac{\mu}{\varepsilon_r}} \frac{\sigma\, \hbar\omega\, \Gamma_{fi} \left|M_{fi}\right|^2}{\left(E_{fi} - \hbar\omega\right)^2 + (\hbar\Gamma_{fi})^2}, \tag{10}$$

where $\hbar\omega$ is the photon energy, μ is the magnetic permeability, ε_r is the dielectric permittivity, and $\sigma = 1/V_{QD}$ is the electron density.

2. Results of numerical calculations and their discussion

This section presents the results of calculations of the electric field's influence on the oscillator strengths of intersubband quantum transitions and the absorption coefficient of electromagnetic waves, performed for both models of lens-shaped quantum dots using formulas (8 – 9). For the model in the form of a spherical segment, calculations of the energy spectrum and wave functions were carried out using the finite element numerical method in the COMSOL Multiphysics system. For the quantum dot model in the form of a flattened hemispheroid, the results obtained using the matrix method and the finite element numerical method agree with high accuracy under different values of the electric field intensity. To ensure an error of less than 0.5 % in the expansion (7), it is sufficient to consider about 10 terms, similar to what was demonstrated for hemispherical quantum dots in [12].

The following parameters of the quantum dot were used for numerical calculations: the effective mass of the electron in *CdS* ($m^* = 0.15\, m_e$, where m_e is the free electron mass), $h = h_e = h_s = 10$ nm, $V_{QD} = 8377.6$ nm^3 the height and volume of the quantum dot.

Table 1 presents the values of the electron energies in states with $n = 1 \div 9$ and $m = 0$, and fig. 2 shows the wave functions of the first 6 states for both models of the lens-shaped quantum dot.

As seen from Table 1, the electron energies in the spherical segment are higher than the corresponding energies in the half-spheroid quantum dot for different values of electric field strength. For excited states, the difference in electron energies is greater, especially for those states where the peaks of the wave function reach the edges of the quantum dot, where the geometry of the considered models differs the most.

Table 1

Electron energies in a lens-shaped quantum dot with $\chi = 2$ *at* $F = 0;\ \pm 300\ kV/cm$.

F(kV/cm)	– 300		0		300	
$E_n^{e,s}$(meV)	hemiellips.	spher.segm.	hemiellips.	spher.segm.	hemiellips.	spher.segm.
E_1	– 127.56	– 124.17	40.31	41.98	156.22	156.92
E_2	– 80.85	– 72.14	70.25	74.93	179.42	181.82
E_3	– 30	– 18.06	111.59	118.14	217.67	220.99
E_4	– 2.62	1.84	136.62	140.03	269.94	272.62
E_5	27.35	40.76	164.87	171.68	285.27	287.57
E_6	54.82	67.51	185.23	195.51	323.84	331.6
E_7	93.45	106.51	230.26	235.5	335.64	336.01
E_8	120.76	140.66	244.52	261.27	376.65	389.69
E_9	150.26	156.26	290.86	295.98	413.88	410.78

Under the influence of an electric field directed along the OZ axis, the peaks of the wave function for all states shift toward the flat boundary of the quantum dot, and the difference $\delta E = E_1^s - E_1^e$ decreases (for the ground state $\varepsilon = 0.4\ \%$ at $F = 300$ kV/cm). In the case of an oppositely directed electric field, the peaks of the wave function shift toward the convex surface of the quantum dot, which differs between these models, and the difference in energies increases (for the ground state $\varepsilon = 2.7\ \%$ at $F = -300$ kV/cm).

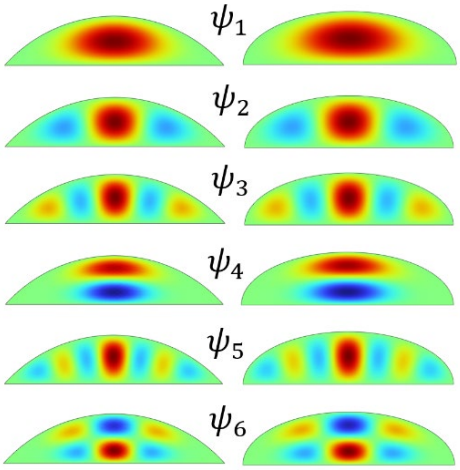

Fig. 2. The appearance of the electron wave functions in states with $n = 1 \div 6$ *and* $m = 0$.

Figure 3 shows the dependence of the oscillator strengths of quantum transitions of an electron in a lens-shaped quantum dot on the electric field strength. Only quantum transitions induced by linearly polarized electromagnetic waves are considered. The direction of light polarization coincides with the direction of the OZ axis. The dependencies $F_{1-f}(F)$ obtained for different models of the lens-shaped quantum dot match with high precision. This can be explained by the fact that only states with small differences in electron energies and wave functions participate in the allowed quantum transitions. The electron wave functions in the spherical segment for these states at $F = 0;\ \pm 300$ kV/cm are shown in the insets.

The figure shows that regardless of the magnitude and direction of the applied electric field, the most probable quantum transition of an electron from the ground state is to the state with two peaks along the OZ axis. This state is characterized by the quantum number $n = 4$, but as the electric field strength directed along the OZ axis increases, due to the anticrossing effect of energy levels, the quantum number of this state becomes equal to 5. The next state into which a quantum transition of the electron is possible is the state with $n = 6$. In the absence of an electric field, the sum of the oscillator strengths for the transitions to the states $n = 4$ and $n = 6$ is 0.98, meaning the probability of other quantum transitions is extremely small. For $F > 0$ the oscillator strength of the quantum transition F_{1-4} decreases, while F_{1-6} increases. Due to the anticrossing effect, at $F = 350$ kV/cm the quantum transition $1 \to 6$ is replaced by the transition $1 \to 7$. As the strength of the electric field directed opposite to the OZ axis increases ($F < 0$), the oscillator strength F_{1-6} decreases to zero, but the probability of a quantum transition to the state $n = 9$. As the electric field strength increases, the probabilities of quantum transitions to higher excited states also increase. The total probability of such transitions at $F = 400$ kV/cm reaches 15 – 20 %.

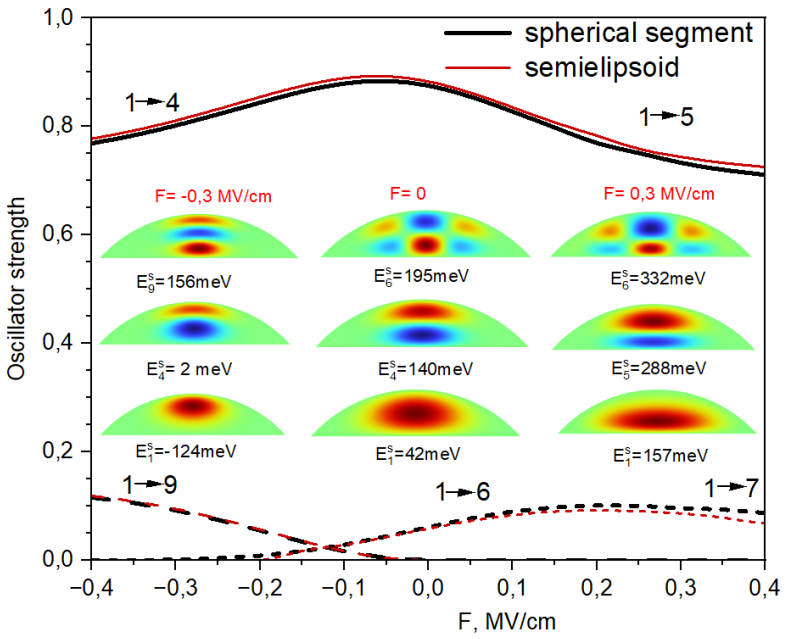

Fig. 3. Dependence of the oscillator strengths of intra-subband quantum transitions of an electron in a lens-shaped quantum dot on the electric field strength (black lines – spherical segment; red lines – half-spheroid quantum dot).

Fig. 4 shows the dependence of the energies of the most probable quantum transitions of an electron on the electric field strength. The electron wave functions in the hemiellipsoid quantum dot at

$F = 0;\ \pm 300$ kV/cm are shown in the insets. As the electric field strength increases, the energies of the quantum transitions rise.

Fig. 5 and fig.6 show the dependencies of the energy spectrum and the oscillator strengths of quantum transitions of an electron on the ratio of the quantum dot's height to the radius of its base $\chi = r_e/h_e$.

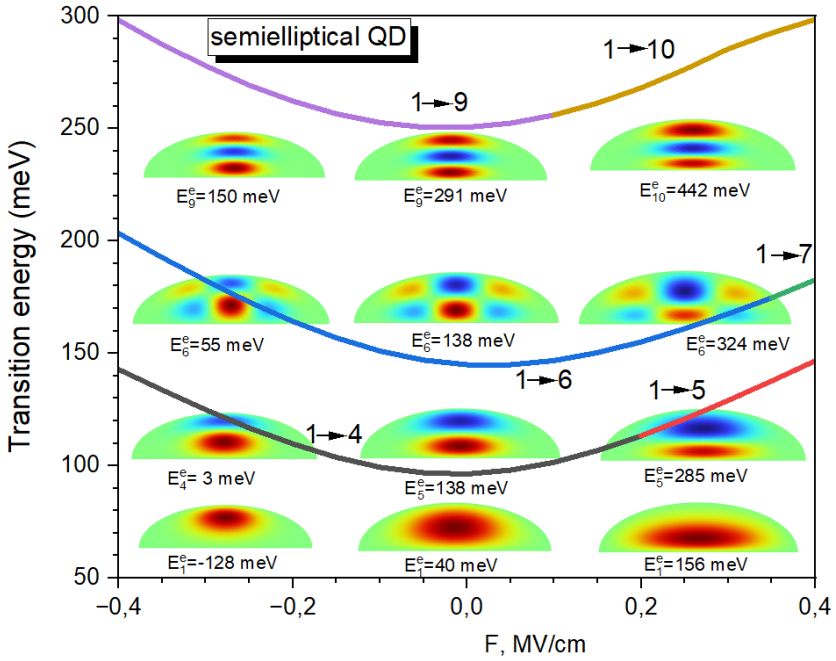

Fig. 4. Dependence of the energies of intra-subband quantum transitions of an electron in a lens-shaped quantum dot on the electric field strength.

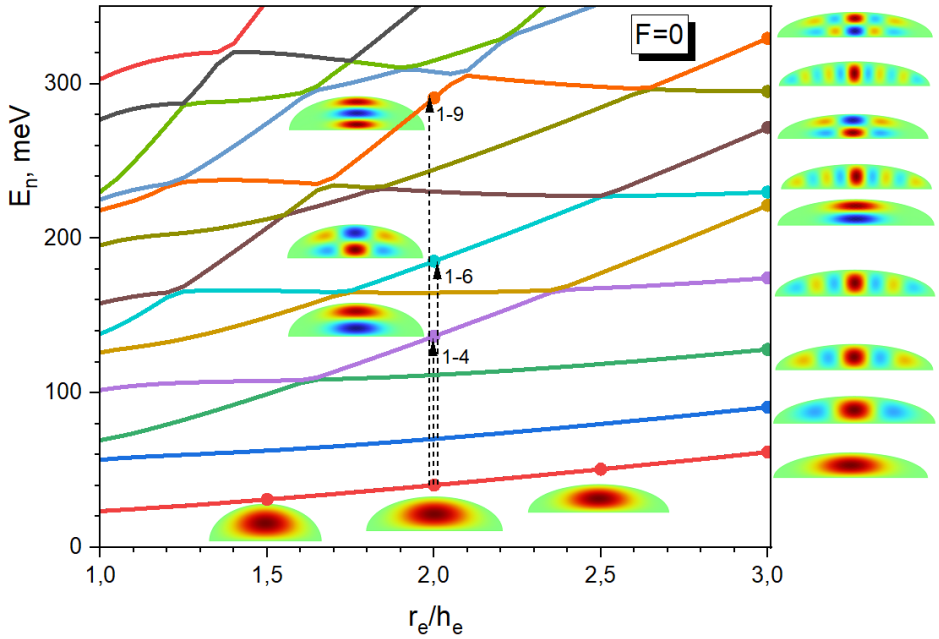

Fig. 5. Dependence of the electron energies in a lens-shaped quantum dot on the ratio $\chi = r_e/h_e$.

From Fig. 5, it can be seen that the energies of the states with $n = 4$, 6, 9, which are the most probable for transitions of an electron excited by a linearly polarized electromagnetic wave, increase sharply as the flattening of the quantum dot increases. At the same time, the oscillator strength of the

main quantum transition increases and quickly approaches saturation with respect to the ratio χ. In the region $1 < \chi < 1.5$, there is a high probability of quantum transitions to the first excited state ($n = 2$), and the oscillator strength $F_{1-5} \to 0$ at $\chi \to 1$.

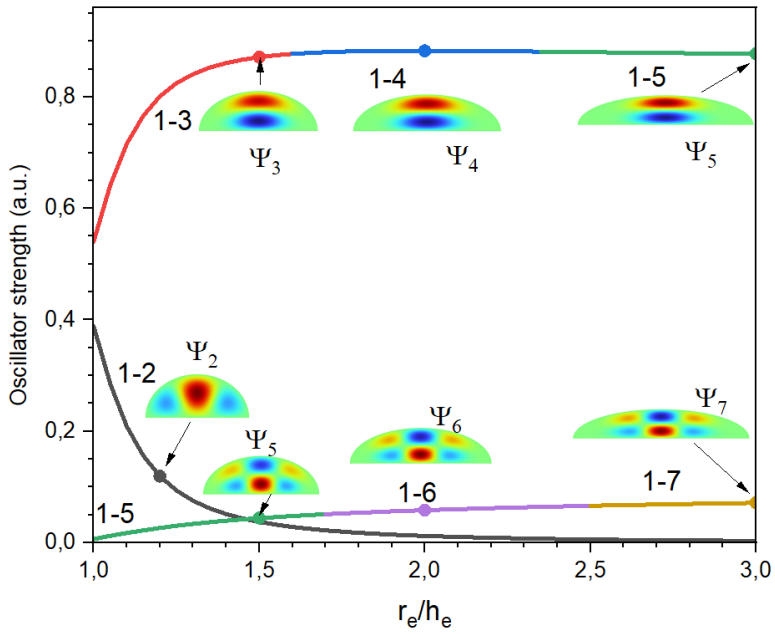

Fig. 6. Dependence of the oscillator strengths of quantum transitions of an electron in a lens-shaped quantum dot on the ratio $\chi = r_e/h_e$.

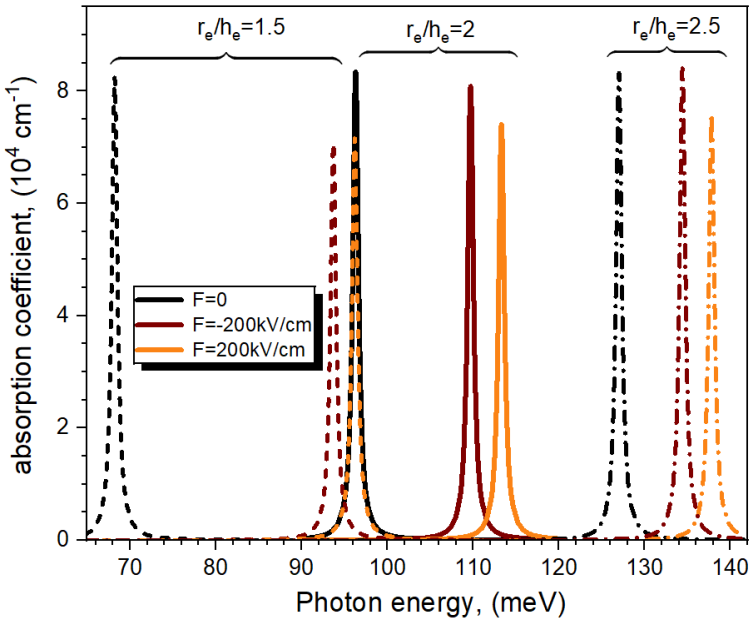

Fig. 7. Dependence of the linear absorption coefficient $\alpha^{(1)}(\omega)$ on the energy of the electromagnetic wave for $\chi = r_e/h_e = 1.5; 2; 2.5$ and $F = 0;\ \pm 200\ kV/cm$.

Fig. 7 shows the dependence of the absorption coefficient on the energy of the electromagnetic wave for a lens-shaped quantum dot with $\chi = 1.5; 2; 2.5$, $F = 0;\ \pm 200$ kV/cm and $\hbar\Gamma_{if} = 1.0$ meV. In

this case, the formula (10) for calculating the absorption coefficient considers only the quantum transition with the largest oscillator strength. Peaks of absorption for different values of electric field strength are shown in different colors, and peaks for quantum dots with different values of the parameter χ are marked with different types of lines. he absorption peak in the absence of an electric field for a quantum dot array with $\chi = 2$ is shown with a solid black line.

As seen from Fig. 7, the height of the peaks does not depend on the ratio χ and only slightly decreases under the influence of an electric field (this is consistent with Figs. 3 and 6). Under the influence of an electric field, the peaks shift to higher energy regions, which is consistent with Fig. 4.

Conclusions

This study presents a theoretical investigation of the impact of an electric field on the optical properties of lens-shaped quantum dots within the effective mass approximation. It was carried out using two models of lens-shaped quantum dots: a spherical segment and a half-ellipsoid quantum dot. To determine the energy levels and wave functions of the electron, the method of expanding the wave function in the basis of exact solutions of the Schrödinger equation without an electric field was used, along with the finite element numerical method in the COMSOL Multiphysics system. It is shown that the energies and oscillator strengths of intra-subband quantum transitions due to the absorption of linearly polarized light, obtained for different models of lens-shaped quantum dots with the same volume and height, match with high precision.

Increasing the flattening of the quantum dot while keeping its volume constant shifts the absorption peaks to higher energy regions but does not affect the oscillator strengths of the quantum transitions. Under the influence of an electric field, the absorption peaks also shift to higher energy regions, but the oscillator strengths of the quantum transitions decrease.

References

1. Holovatsky V., Chubrei M., Yurchenko O. (2021) Impurity Photoionization Cross-Section and Intersubband Optical Absorption Coefficient in Multilayer Spherical Quantum Dots. *Phys Chem solid state.* 4 (4), 630 – 637.
2. Holovatsky V., Holovatskyi I., Yakhnevych M. (2018) Joint effect of electric and magnetic field on electron energy spectrum in spherical nanostructure *ZnS*/*CdSe*/*ZnS*. Phys E Low-Dimensional Syst Nanostructures. 104, 58 – 63.
3. Holovatsky V., Chubrei M., Duque C. (2022) Core-shell type-II spherical quantum dot under externally applied electric field. Thin Solid Films. 747, 139142.
4. Holovatsky V., Holovatska N., Chubrei M. (2021) Optical absorption, photoionization and binding energy of shallow donor impurity in spherical multilayered quantum dot. Proceedings of SPIE – The International Society for Optical Engineering. 12126, 1212603. doi:10.1117/12.2614673
5. Gurioli M., Wang Z., Rastelli A., Kuroda T., Sanguinetti S. (2019) Droplet epitaxy of semiconductor nanostructures for quantum photonic devices. Nat Mater. 18 (8), 799 – 810.
6. Nemcsics A. Quantum Dots Prepared by Droplet Epitaxial Method. In: Quantum Dots – Theory and Applications. InTech; 2015:119 – 148. doi:10.5772/60823
7. Li R., Liu F., Lu Q. (2023) Quantum Light Source Based on Semiconductor Quantum Dots: A Review. *Photonics*. 10 (6), 639.
8. Lorenzi B, Chen G. (2018) Theoretical efficiency of hybrid solar thermoelectric-photovoltaic generators. *J Appl Phys*., 124 (2), 0 – 13.

9. Urban JJ. (2015) Prospects for thermoelectricity in quantum dot hybrid arrays. *Nat Publ Gr.* 10 (12), 997 – 1001.
10. Wu S. (2021) Anisotropic exciton Stark shift in hemispherical quantum dots. *Chinese Phys B*. 30 (5), 053201.
11. Lopez Gondar J., Costa B., Trallero-Giner C., Marques G. (2002) Zeeman Effect in Self-Assembled Quantum Dots. Phys status solidi. 230 (2), 437 – 442.
12. Holovatsky, V. A., Holovatskyi, I. V., & Duque, C. A. (2024). Electric field effect on the absorption coefficient of hemispherical quantum dots. *Molecular Crystals and Liquid Crystals*, 1 – 11.
13. Cantele G., Ninno D., Iadonisi G. (2000) Confined states in ellipsoidal quantum dots. *J Phys Condens Matter*. 12 (42), 9019 – 9036.
14. Cantele G., Ninno D., Iadonisi G. (2001) Calculation of the Infrared Optical Transitions in Semiconductor Ellipsoidal Quantum Dots. *Nano Lett*. 1 (3), 121 – 124.
15. Hértilli S., Yahyaoui N., Zeiri N., Baser P., Said M., Saadaoui S. (2024) Theoretical modeling of nonlinear optical properties in spheroidal *CdTe*/*ZnTe* core/shell quantum dot embedded in various dielectric matrices. *Results Phys*. 56.

Submitted: 13.03.2024.

Головацький В.А., *доктор фіз.-мат. наук*
Головацький І.В.
Головацька Н.Г.

Чернівецький національний університет імені Юрія Федьковича,
вул. Коцюбинського 2, Чернівці, 58012, Україна
e-mail: v.holovatsky@chnu.edu.ua

ВПЛИВ ЕЛЕКТРИЧНОГО ПОЛЯ НА ВНУТРІШНЬОЗОННЕ ОПТИЧНЕ ПОГЛИНАННЯ ЛІНЗОПОДІБНИХ КВАНТОВИХ ТОЧОК

В роботі досліджено вплив електричного поля на енергії, сили осцилятора та коефіцієнт поглинання внутрішньозонних квантових переходів електрона в лінзоподібних квантових точках. Задача розв'язувалась в рамках наближення ефективної маси для двох моделей лінзоподібної квантової точки: кульовий сегмент та половина сплющеного еліпсоїда. Для обох моделей дослідження виконано методом кінцевих елементів в системі COMSOL Multiphysics. Крім цього, для другої моделі квантової точки отримано точні розв'язки рівняння Шредінгера, на основі яких досліджено вплив електричного поля методом діагоналізації. Показано, що енергії та сили осциляторів внутрішньозонних квантових переходів, що отримані різними методами та для різних моделей лінзоподібної квантової точки збігаються з високою точністю.

Ключові слова: лінзоподібна квантова точка, еліпсоїдна квантова точка, коефіцієнт поглинання.

Література

1. Holovatsky V., Chubrei M., Yurchenko O. (2021) Impurity Photoionization Cross-Section and Intersubband Optical Absorption Coefficient in Multilayer Spherical Quantum Dots. *Phys Chem*

solid state. 4 (4), 630 – 637.
2. Holovatsky V., Holovatskyi I., Yakhnevych M. (2018) Joint effect of electric and magnetic field on electron energy spectrum in spherical nanostructure *ZnS*/*CdSe*/*ZnS*. Phys E Low-Dimensional Syst Nanostructures. 104, 58 – 63.
3. Holovatsky V., Chubrei M., Duque C. (2022) Core-shell type-II spherical quantum dot under externally applied electric field. Thin Solid Films. 747, 139142.
4. Holovatsky V., Holovatska N., Chubrei M. (2021) Optical absorption, photoionization and binding energy of shallow donor impurity in spherical multilayered quantum dot. Proceedings of SPIE – The International Society for Optical Engineering. 12126, 1212603. doi:10.1117/12.2614673
5. Gurioli M., Wang Z., Rastelli A., Kuroda T., Sanguinetti S. (2019) Droplet epitaxy of semiconductor nanostructures for quantum photonic devices. Nat Mater. 18 (8), 799 – 810.
6. Nemcsics A. Quantum Dots Prepared by Droplet Epitaxial Method. In: Quantum Dots – Theory and Applications. InTech; 2015:119 – 148. doi:10.5772/60823
7. Li R., Liu F., Lu Q. (2023) Quantum Light Source Based on Semiconductor Quantum Dots: A Review. *Photonics*. 10 (6), 639.
8. Lorenzi B, Chen G. (2018) Theoretical efficiency of hybrid solar thermoelectric-photovoltaic generators. *J Appl Phys*., 124 (2), 0 – 13.
9. Urban JJ. (2015) Prospects for thermoelectricity in quantum dot hybrid arrays. *Nat Publ Gr.* 10 (12), 997 – 1001.
10. Wu S. (2021) Anisotropic exciton Stark shift in hemispherical quantum dots. *Chinese Phys B*. 30 (5), 053201.
11. Lopez Gondar J., Costa B., Trallero-Giner C., Marques G. (2002) Zeeman Effect in Self-Assembled Quantum Dots. Phys status solidi. 230 (2), 437 – 442.
12. Holovatsky, V. A., Holovatskyi, I. V., & Duque, C. A. (2024). Electric field effect on the absorption coefficient of hemispherical quantum dots. *Molecular Crystals and Liquid Crystals*, 1 – 11.
13. Cantele G., Ninno D., Iadonisi G. (2000) Confined states in ellipsoidal quantum dots. *J Phys Condens Matter*. 12 (42), 9019 – 9036.
14. Cantele G., Ninno D., Iadonisi G. (2001) Calculation of the Infrared Optical Transitions in Semiconductor Ellipsoidal Quantum Dots. *Nano Lett*. 1 (3), 121 – 124.
15. Hértilli S., Yahyaoui N., Zeiri N., Baser P., Said M., Saadaoui S. (2024) Theoretical modeling of nonlinear optical properties in spheroidal *CdTe*/*ZnTe* core/shell quantum dot embedded in various dielectric matrices. *Results Phys*. 56.

Надійшла до редакції: 13.03.2024.